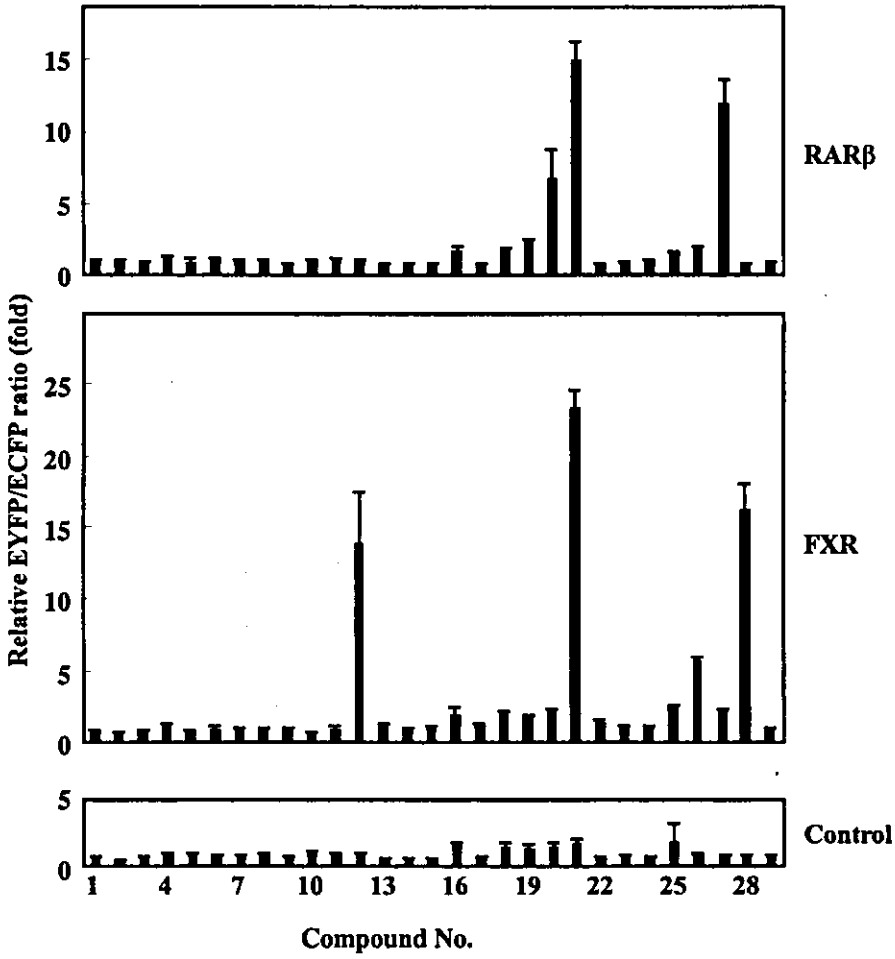
15
10
5
0
RARβ
25
20
15
10
5
0
FXR
5
0
Control
Relative EYFP/ECFP ratio (fold)
1
4
7
10
13
16
19
22
25
28
Compound No.

(A)

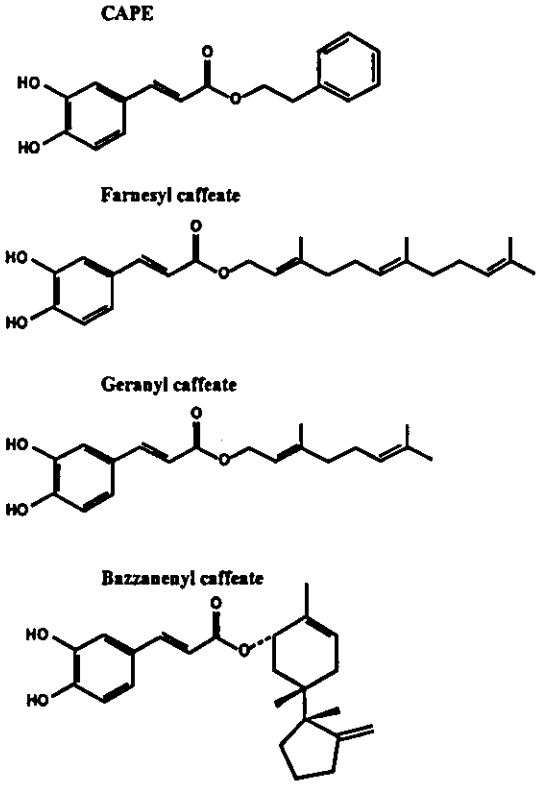
CAPE
Farnesyl caffeate
Geranyl caffeate
Bazzanenyl caffeate

(B)

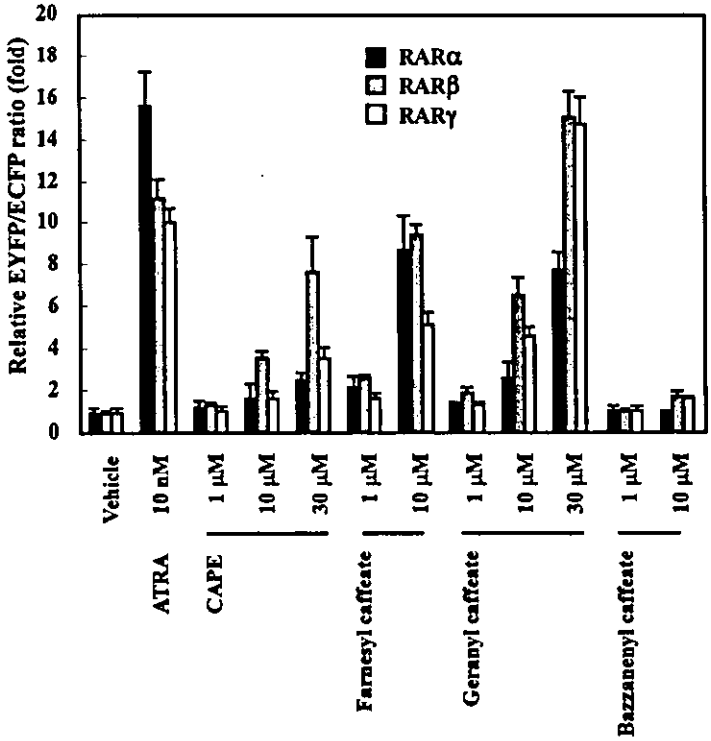
Relative EYFP/ECFP ratio (fold)
RARα
RARβ
RARγ
Vehicle
10 nM
1 μM
10 μM
30 μM
1 μM
10 μM
1 μM
10 μM
30 μM
1 μM
10 μM
ATRA
CAPE
Farnesyl caffeate
Geranyl caffeate
Bazzanenyl caffeate

(A)

Ginkgolic acid 15:1

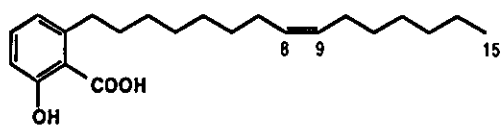

Ginkgolic acid 17:1

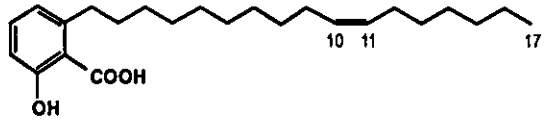

Ginkgolic acid 15:0

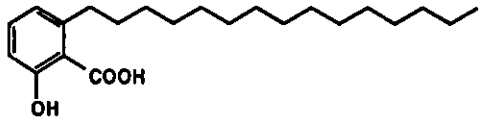

Ginkgolic acid 13:0

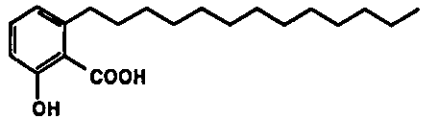

2-methyl ginkgolic acid methyl ester

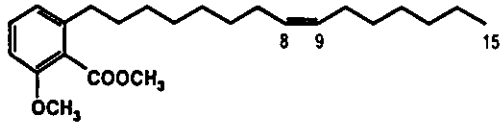

Grifolin

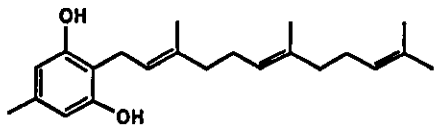

(B)

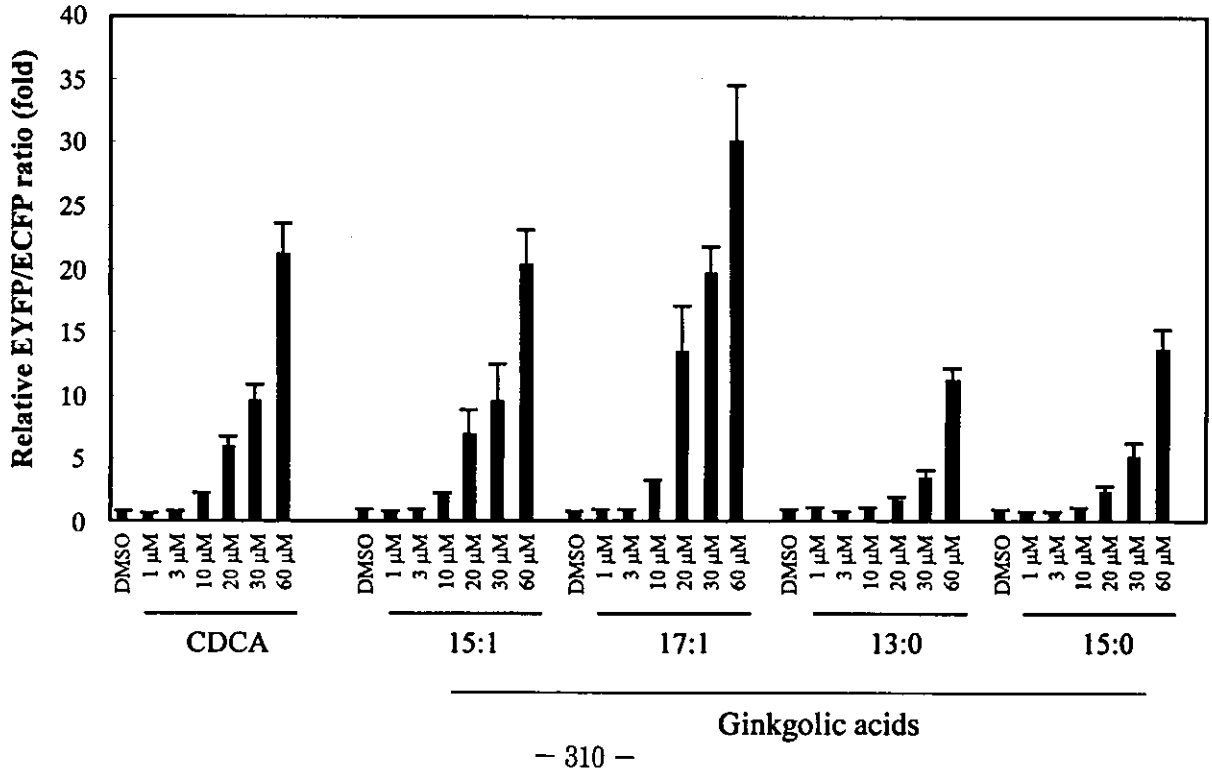

J Pharmacol Sci 96, 499 – 501 (2004)

Journal of Pharmacological Sciences

Rapid Communication

The *R*(–)-Enantiomer of Efonidipine Blocks T-type but Not L-type Calcium Current in Guinea Pig Ventricular Myocardium

Hikaru Tanaka[1,*], Chisa Komikado[1], Hideaki Shimada[1], Kentaro Takeda[1], Iyuki Namekata[1], Toru Kawanishi[2], and Koki Shigenobu[1]

[1]*Department of Pharmacology, Toho University School of Pharmaceutical Sciences, Chiba 274-8510, Japan*
[2]*Division of Biological Chemistry and Biologicals, National Institute of Health Sciences, Tokyo 158-8501, Japan*

Received November 16 2004; Accepted November 24, 2004

Abstract. In guinea pig ventricular cardiomyocytes, the *R*(–)-enantiomer of efonidipine concentration-dependently blocked T-type Ca^{2+} current with 85% inhibition at 1 μM. In contrast, *R*(–)-efonidipine (1 μM) had no effect on the L-type Ca^{2+} current and Ca^{2+} transient in cardiomyocytes and contractile force in papillary muscles. Thus, *R*(–)-efonidipine is a highly selective blocker of the T-type Ca^{2+} current in native myocardia.

Keywords: *R*(–)-efonidipine, T-type Ca^{2+} channel, cardiomyocyte

The T-type Ca^{2+} channel has properties different from those of the L-type such as a more negative voltage range of activation and inactivation, rapid gating kinetics, and resistance to standard Ca^{2+} blockers (1, 2). Three cDNAs for T-type Ca^{2+} channels have been cloned and studies have begun on the structure and function of the channel. T-type Ca^{2+} channels are considered to participate in normal and abnormal cardiac automaticity, regulation of vascular tone, and hormone secretion. Involvement of T-type Ca^{2+} channels in cell growth and proliferation has been proposed and the distribution and properties of T-type Ca^{2+} channels are reported to be altered in pathophysiological conditions such as ventricular hypertrophy and cardiomyopathy. Thus, the T-type Ca^{2+} channel is now considered to be a novel therapeutic target for various cardiovascular disorders. However, blockers of the T-type Ca^{2+} channel with sufficient potency and selectivity has not yet been developed. We have found that efonidipine, a 1,4-dihydropyridine Ca^{2+} channel blocker with a phosphonate moiety (3), has dual blocking effects on L-type and T-type Ca^{2+} currents (4, 5), which underlies its unique clinical profiles (6). Recently, Furukawa et al. (7) reported that the *R*(–)-enantiomer of efonidipine blocks the T-type Ca^{2+} channel much more potently than the L-type based on voltage clamp experiments with recombinant Ca^{2+} channels expressed in *Xenopus* oocytes and baby hamster kidney cells. To clarify if *R*(–)-efonidipine could be used as a specific inhibitor of the T-type Ca^{2+} channel in native myocardium, we examined its effect on T-type and L-type Ca^{2+} currents in isolated guinea pig myocardium.

The present study was conducted in accordance with the "Guiding Principles for the Care and Use of Laboratory Animals Approved by The Japanese Pharmacological Society". Standard voltage-clamp experiments were performed with ventricular cardiomyocytes as described earlier (5, 8). The L-type Ca^{2+} current was elicited every 10 s by 300-ms depolarizing test pulses from a holding potential of –40 to +10 mV. The T-type Ca^{2+} current was elicited every 10 s by 200-ms depolarizing test pulses to –30 mV in the presence of 10 μM tetrodotoxin; the membrane potential between episodes was kept at –40 mV until the holding potential of –80 mV was applied at 2.5 s prior to the depolarizing pulse. Intracellular Ca^{2+} concentration was measured in indo-1(AM)-loaded guinea pig ventricular myocytes with a fluorescence imaging system (Aquacosmos; Hamamatsu Photonics, Hamamatsu), and analyzed as described earlier (9). Contractile force measurements were performed with isolated right ventricular papillary muscles as described earlier (5). At 60 min before the addition of drugs, the solution in the organ bath was changed to a high K^+ solution in order to increase the Ca^{2+} sensitivity of the contraction; KCl was increased to 30 mM and $CaCl_2$ to 5 mM, and 100 μM isobutylmethylxantine and 1 μM tetrodotoxin were added. *R*(–)-

*Corresponding author. FAX: +81-47-472-2113
E-mail: htanaka@phar.toho-u.ac.jp

Efonidipine and *S*(+)-efonidipine were provided by Nissan Chemical Industries, Ltd. (Tokyo). To exclude the effect of vehicle (dimethyl sulfoxide, final concentration 0.05%) and time dependent decay of the parameters measured, the obtained values were normalized by the corresponding data obtained in control experiments performed with vehicle only. All data were presented as the mean ± S.E.M. Statistical significance between means was evaluated by Student's *t*-test. *P* values less than 0.05 were considered significant.

The T-type Ca^{2+} current had a peak current density of 0.61 ± 0.05 pA/pF (n = 23) and was completely blocked by 40 μM nickel (not shown). *R*(−)-Efonidipine (1 μM) blocked the T-type Ca^{2+} current by 85% (Fig. 1Aa). The inhibition of T-type Ca^{2+} current by *R*(−)-efonidipine, at 10 nM to 1 μM, was concentration-dependent (Fig. 1B). The L-type Ca^{2+} current had a peak current density of 7.00 ± 0.42 pA/pF (n = 29) and was completely blocked by 1 μM nifedipine (not shown). *R*(−)-Efonidipine had no effect on the L-type Ca^{2+} current at 1 μM (Fig. 1Ab, 1B). Partial inhibition was observed at 10 μM (Fig. 1B). In voltage clamped cardiomyocytes, *R*(−)-efonidipine (1 μM) had no significant effect on the L-type Ca^{2+} current (Fig. 1), while 1 μM *S*(+)-efonidipine blocked the current by 95% (Fig. 2B). *R*(−)-Efonidipine (1 μM)

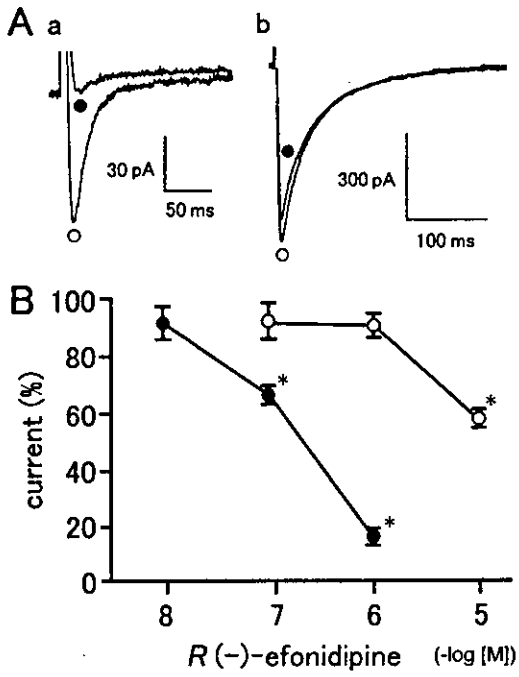

Fig. 1. Effect of *R*(−)-efonidipine on T-type and L-type Ca^{2+} currents. A: Typical current traces of T-type (a) and L-type (b) Ca^{2+} currents obtained in the absence (open circles) or presence (closed circles) of 1 μM *R*(−)-efonidipine. B: Concentration-response curves for the inhibitory effects of *R*(−)-efonidipine on the T-type (closed circles) and L-type (open circles) Ca^{2+} currents. Peak inward current amplitude of the L-type and T-type Ca^{2+} currents in the presence of *R*(−)-efonidipine was expressed as a percentage of the corresponding value in the presence of vehicle only. Symbols and vertical bars indicate the mean ± S.E.M. from four to five experiments: * indicates significant difference ($P<0.05$) from the corresponding current measurements in the presence of vehicle only.

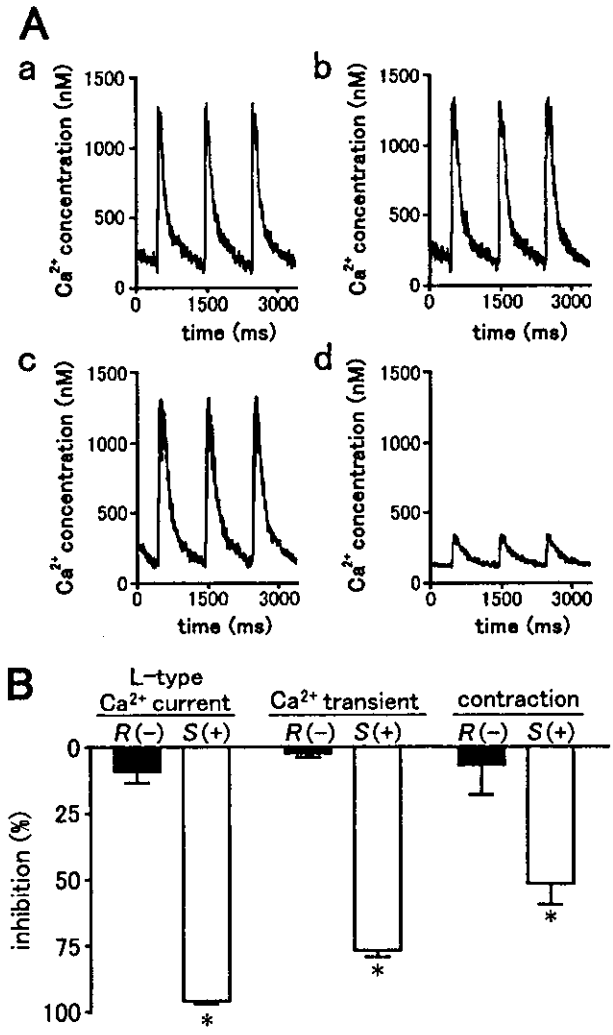

Fig. 2. Lack of L-type Ca^{2+} current blockade by 1 μM *R*(−)-efonidipine. A: Typical Ca^{2+} transients obtained in the absence (a, c) or presence of 1 μM *R*(−)-efonidipine (b) and *S*(+)-efonidipine (d). B: Summarized results for the inhibitory effects of 1 μM *R*(−)-efonidipine (closed columns) and 1 μM *S*(+)-efonidipine (open columns) on the L-type Ca^{2+} current and Ca^{2+} transient in isolated ventricular cardiomyocytes and contraction of partially depolarized papillary muscles. Ca^{2+} transients and contractions were evoked by field stimulation of 3-ms duration and 1.5 times threshold voltage. Inhibition by *R*(−)-efonidipine or *S*(+)-efonidipine of each parameter was expressed as a percentage of the corresponding value in the presence of vehicle only. Columns and vertical bars indicate the mean ± S.E.M. from four to six experiments. * indicates significant difference ($P<0.05$) from corresponding values in the absence of drugs (vehicle only).

had no effect on the Ca^{2+} transient, while significant reduction was observed with 1 μM *S*(+)-efonidipine (Fig. 2: A and B). In partially depolarized papillary muscle preparations, 1 μM *R*(−)-efonidipine had no effect on the contractile force, while significant reduction was observed with 1 μM *S*(+)-efonidipine (Fig. 2B).

R(−)-Efonidipine was shown to selectively block the T-type Ca^{2+} current in native myocardial cells (Fig. 1). Blockade of the L-type Ca^{2+} current was negligible at 1 μM, a concentration at which T-type Ca^{2+} current was blocked by 85%. That *R*(−)-efonidipine (1 μM) had no effect on the Ca^{2+} transient and contractile force (Fig. 2) also indicates lack of blocking effect on the L-type Ca^{2+} current. In contrast, *S*(+)-efonidipine markedly inhibited the L-type Ca^{2+} current, Ca^{2+} transient, and contractile force (Fig. 2). Thus, the L-type Ca^{2+} channel blocking activity of (±)-efonidipine (5) could be attributed to the *S*(+)-enantiomer. In the present voltage-clamp experiments, the membrane potential between depolarizing test pulses were kept at −40 mV both for T-type and L-type Ca^{2+} current measurements. However, to elicit the T-type Ca^{2+} current, a holding potential of −80 mV had to be applied for 2.5 s before the test pulse. As the blockade of T-type Ca^{2+} channel by efonidipine is dependent on stimulation frequency (10) and voltage (7), the 30-fold selectivity towards T-type Ca^{2+} channels observed may be an underestimate; the selectivity may be higher in the in vivo condition where T-type and L-type Ca^{2+} channels share a common membrane potential. (±)-Efonidipine (10 μM) was reported to have no siginificant blocking effect on recombinant N-type, P-type, and Q-type Ca^{2+} channels (7). The delayed rectifier potassium current (I_K) and inward rectifier potassium current (I_{K1}) were not affected by 10 μM (±)-efonidipine (5). Thus, *R*(−)-efonidipine appears to be a specific inhibitor of the T-type Ca^{2+} channel so far, and it would be useful for further studies on T-type Ca^{2+} channels and development of a novel pharmacological therapy.

References

1 Ertel S, Ertel A. Low-voltage-activated T-type Ca^{2+} channels. Trends Pharmacol Sci. 1997;18:37–42.

2 Perez-Reyes E. Molecular physiology of low-voltage-activated t-type calcium channels. Physiol Rev. 2003;83:117–161.

3 Masuda Y, Tanaka S. Efonidipine hydrochloride: a new calcium antagonist. Cardiovasc Drug Rev. 1994;12:123–135.

4 Masumiya H, Tanaka H, Shigenobu K. Effects of Ca^{2+} channel antagonists on sinus node: prolongation of late phase 4 depolarization by efonidipine. Eur J Pharmacol. 1997;335:15–21.

5 Masumiya H, Shijyuku T, Tanaka H, Shigenobu K. Inhibition of myocardial T- and L-type Ca^{2+} currents by efonidipine: possible mechanism for its chronotropic effect. Eur J Pharmacol. 1998;349:351–357.

6 Tanaka H, Shigenobu K. Efonidipine hydrochloride: a dual blocker of L- and T-type Ca^{2+} channels. Cardiovasc Drug Rev. 2002;20:81–92.

7 Furukawa T, Miura R, Honda M, Kamiya N, Mori Y, Takeshita S, et al. Identification of *R*-(−)-isomer of efonidipine as a selective blocker of T-type Ca^{2+} channels. Br J Pharmacol. 2004;143:1050–1057.

8 Takeda K, Yamagishi R, Masumiya H, Tanaka H, Shigenobu K. Effect of cilnidipine on L- and T-type calcium currents in guinea pig ventricle and action potential in rabbit sinoatrial node. J Pharmacol Sci. 2004;95:398–401.

9 Tanaka H, Kawanishi T, Kato Y, Nakamura R, Shigenobu K. Restricted propagation of cytoplasmic Ca^{2+} oscillation into the nucleus in guinea pig cardiac myocytes as revealed by rapid scanning confocal microscopy and indo-1. Jpn J Pharmacol. 1996;70:235–242.

10 Masumiya H, Kase J, Tanaka Y, Tanaka H, Shigenobu K. Frequency-dependent blockade of T-type Ca^{2+} current by efonidipine in cardiomyocytes. Life Sci. 2000;68:345–351.

Journal of Pharmacological Sciences

Full Paper

Simultaneous Real-Time Detection of Initiator- and Effector-Caspase Activation by Double FRET Analysis

Hiroshi Kawai[1,*], Takuo Suzuki[1], Tetsu Kobayashi[1], Haruna Sakurai[2], Hisayuki Ohata[2], Kazuo Honda[2], Kazutaka Momose[2], Iyuki Namekata[3], Hikaru Tanaka[3], Koki Shigenobu[3], Ryu Nakamura[4], Takao Hayakawa[1], and Toru Kawanishi[1]

[1]*Division of Biological Chemistry and Biologicals, National Institute of Health Sciences, Tokyo 158-8501, Japan*
[2]*Department of Pharmacology, School of Pharmaceutical Sciences, Showa University, Tokyo 142-8555, Japan*
[3]*Department of Pharmacology, Toho University School of Pharmaceutical Sciences, Chiba 274-8510, Japan*
[4]*Carl Zeiss Co., Ltd., Tokyo 160-0003, Japan*

Received August 31, 2004; Accepted January 8, 2005

Abstract. Fluorescence resonance energy transfer (FRET) with green fluorescent protein (GFP) variants has become widely used for biochemical research. In order to expand the choice of fluorescent range in FRET analysis, we designed various color versions of the FRET-based probes for caspase activity, in which the substrate sequence of the caspase was sandwiched by donor and acceptor fluorescent proteins, and studied the potential of these color versions as fluorescent indicators. Six color versions were constructed by a combination of Cyan fluorescent protein (CFP), GFP, yellow fluorescent protein (YFP), and DsRed. Real-time monitoring in single cells revealed that all probes could detect caspase activation during tumor necrosis factor (TNF)-α-induced cell death as a fluorescent change. GFP-DsRed and YFP-DsRed were as sensitive as CFP-YFP, and CFP-DsRed also showed a large fluorescent change. By using two probes, CFP-DsRed and YFP-DsRed, we carried out simultaneous multi-FRET analysis and revealed that the initiator- and effector-caspases were activated almost simultaneously in TNF-α-induced cell death. These findings may give experimental bases for the development of novel techniques to analyze multi-events simultaneously in single cells by using FRET probes in combination.

Keywords: fluorescence resonance energy transfer, green fluorescent protein, tumor necrosis factor-α, cell death, caspase

Introduction

Many probes for various physiological reactions have been developed with green fluorescent protein (GFP) variants by using a similar strategy as that used with cameleon, the Ca^{2+}-sensing fusion protein developed by Miyawaki et al. (1 – 9). The cameleon consists of cyan fluorescent protein (CFP), calmodulin, M13 peptide, and yellow fluorescent protein (YFP). This fusion protein senses Ca^{2+} as the change of fluorescence resonance energy transfer (FRET) efficiency between CFP and YFP. Calmodulin binds M13 in the presence of Ca^{2+}, which causes conformational change in cameleon, resulting in a change in the distance between and relative orientation of CFP and YFP. This change alters the FRET efficiency from CFP to YFP; therefore, Ca^{2+} can be monitored as the fluorescent change (1).

CFP and YFP are the most frequently used pair for analysis by FRET. This pair is suitable for FRET analysis because the spectral overlap between the emission of the donor protein (CFP) and the excitation of the acceptor protein (YFP) is sufficient for energy transfer, and their ranges of fluorescence are far apart enough to be separated by measuring devices such as fluorescent microscopy (10). However, there are limitations for the CFP-YFP pair. It is impossible, for example, to use the CFP-YFP FRET probe for simultaneous measurement with other probes that are made of GFP variants or have

*Corresponding author. FAX: +81-3-3700-9084
E-mail: kawai@nihs.go.jp.

fluorescein structure. If more choice of FRET probes is available from wider fluorescence ranges, it would allow us to analyze multi-events simultaneously occurring in living cells.

In this paper, we developed caspase-sensors of various colors by using cyan, green, yellow, and red fluorescent proteins and assessed their ability to detect the caspase activation in living single cells. Based on the findings obtained, we tried to perform multi-event FRET analysis and clarify the temporal relationships between biochemical reactions during cell death.

Materials and Methods

Plasmid construction

Plasmid encoding CY-sensor, YFP-peptide-CFP, was generated as previously reported (11). The sequence encoding 11 amino acids at the C-terminus of YFP was eliminated in this construct. The C-terminal truncated forms of the CFP (or GFP) gene were generated by PCR with primers containing the NheI site or BspEI site and pECFP-C1 (or pEGFP-C1; Clontech, Palo Alto, CA, USA) as a template, and the restricted fragment was inserted into the NheI/BspEI sites of the CY-sensor to generate a plasmid carrying truncated CFP (or GFP) at the N-terminus. DsRed was generated from pDsRed2-C1 (Clontech) by PCR, at the AgeI/NotI sites, and the restricted fragment was inserted into the AgeI/NotI sites of the CY-sensor to generate a plasmid carrying DsRed2 at the C-terminus. CG-, CR-, GR-, and YR-sensors were generated with a combination of these elements. The AgeI/BsrGI fragment from pEGFP-C1 was inserted into the AgeI/BsrGI sites of the CY-sensor to generate the GY-sensor. All cloned sequences were verified by sequencing.

Cell culture and transfection

HeLa cells were cultured in DMEM (Sigma-Aldrich, St. Louis, MO, USA) supplemented with 100 units/ml of penicillin G, 100 μg/ml of streptomycin, and 10% fetal calf serum (Gibco). Plasmid encoding the sensor protein was transfected into HeLa cells using Effectene Transfection Reagent (Qiagen, Hilden, Germany) according to the manufacturer's instructions. After 12 – 24 h incubation with the transfection reagent, the cells were washed with PBS and cultivated on dishes suitable for assay in medium containing 500 μg/ml of G418 for an additional 1 – 3 days until the assay was performed.

Western blotting

Cells cultured in a plastic dish were washed with PBS and lysed with 1 × SDS loading buffer. The samples dissolved in 1 × SDS loading buffer were incubated at 95°C for 2 min, and then they were loaded onto SDS-polyacrylamide gels (10%). Proteins were separated at 20 mA and then blotted to PVDF membranes in Tris-glycine transfer buffer at 100 V for 2 h. The membrane was incubated with block ace (Dainippon Pharmaceutical, Osaka) for 1 h, anti-GFP peptide antibody (Clontech, diluted with 0.1 × block ace to 1:1,000) for 2 h, and anti-rabbit IgG horseradish peroxidase-conjugated secondary antibody (Chemicon International Inc., Temecula, CA, USA; diluted with 0.1 × block ace to 1:10,000) for 1 h. The membrane was washed with TBS-T 3 times for 5 min after the incubation with the antibody. All of these incubations were performed at room temperature. The membrane was developed with the ECL chemiluminescence detection reagent (Amersham Biosciences, Piscataway, NJ, USA).

Measurement of fluorescent spectra of the sensors in HeLa cells

Spectral imaging was performed with LSM510META (Carl Zeiss) (12). Cells expressing one of the sensors were observed by excitation light at 458 nm (Ar laser), emitted fluorescence was separated by a grating, and the separated fluorescence were detected by 24 photomultiplier tubes (PMT) that were set to detect fluorescence at 468 – 714 nm. Each PMT detected fluorescence in the 10.7-nm wavelength range. So, the fluorescent spectrum at 468 – 714 nm was obtained with 10.7-nm resolution. Cell death was induced by incubation with tumor necrosis factor (TNF)-α (100 ng/ml) and cycloheximide (CHX, 10 μg/ml) for 6 h. Fluorescent spectra of living and dead cells were obtained from the whole cell region of normal-shaped and spherical cells, respectively.

Real-time imaging with FRET sensors

Transfected cells were cultured on a cover glass (25-mm diameter, 0.15 – 0.18-mm thickness) for 1 – 3 days. Cells were treated with TNF-α/CHX and then incubated under the usual culture condition for 1 – 2 h before analysis. Analyses were carried out by confocal laser-scanning fluorescent microscopy using a Carl Zeiss LSM510 system. During the observation, the media were buffered with 10 mM hepes buffer (pH 7.4), and the cells were maintained at 35 – 37°C. DIC images and grayscale images for fluorescence channels were obtained every 2 min unless otherwise described. Excitation lights for the FRET probe (458 nm for the CG-, CY-, GY-, and CR-sensors; 488 nm for the GR- and YR-sensors) were provided by an Ar laser with a 458 or 488 dichroic mirror. Images of the FRET probe were obtained separately for both donor and acceptor fluorescence using a dichroic mirror and band-pass

Table 1. Measurement conditions for real-time analysis by LSM510

Sensor	Fusion protein[a]	Excitation (nm)[b]	Emission (nm)[c]		
			beam splitter	emission filter	
				donor	acceptor
CG	GFP-peptide-CFP	458	515	467.5 – 497.5	515 – 545
CY	YFP-peptide-CFP	458	515	467.5 – 497.5	515 – 545
GY	YFP-peptide-GFP	458	515	475 – 525	515 – 545
CR	CFP-peptide-DsRed	458	515	467.5 – 497.5	560 – 615
GR	GFP-peptide-DsRed	488	545	505 – 530	560 – 615
YR	YFP-peptide-DsRed	488	545	505 – 530	560 – 615

[a]N-terminal C/G/YFP were in a truncated form in which 11 amino acids at the C-terminus were eliminated, and His_{10} was present at the C-terminus of CG, CY, and GY. [b]Excitation light was obtained by Ar laser and a 458 or 488 dichroic mirror. [c]Emitted fluorescence was separated by a 515 or 545 dichroic mirror, and the fluorescence of the donor and that of the acceptor were obtained through band pass emission filters.

emission filters as shown in Table 1. Images were processed and quantified using MetaFluor software as follows: The average pixel intensity of the fluorescence of the whole cell region was determined for each channel. The ratio value was calculated as the average pixel value of the fluorescent ratio, (fluorescent intensity for the acceptor channel) / (fluorescent intensity for the donor channel), in the whole cell region. As cells changed their morphology during the observation, the whole cell region was determined separately in each image.

Results

Construction and characterization of FRET probes

We developed plasmids expressing caspase sensors as shown in Fig. 1a. A 12-amino-acid peptide derived from poly(ADP-ribose)polymerase (PARP) that is a well-known substrate of effector caspases was sandwiched by two different fluorescent proteins (an example of CFP-YFP is shown in Fig. 1a). The peptide sequence contains a caspase recognition site in the middle, and this fusion protein was cleaved mainly by caspase-3 (11). CFP-GFP, CFP-YFP, GFP-YFP, CFP-DsRed, GFP-DsRed, and YFP-DsRed were used as the donor-acceptor pairs. We named these fusion proteins CG-, CY-, GY-, CR-, GR-, and YR-sensor, respectively (Table 1). These fusion proteins show FRET in their intact form, whereas in the presence of active caspase, the peptide sequence is cleaved, CFP and YFP are far apart, and the fusion proteins do not show FRET any longer. The fluorescent ratio of acceptor/donor reflects the amount of FRET, so we used the reduction of this value as an index of caspase activation.

HeLa cells expressing one of these fusion proteins were treated with TNF-α/CHX. After 6-h exposure, the

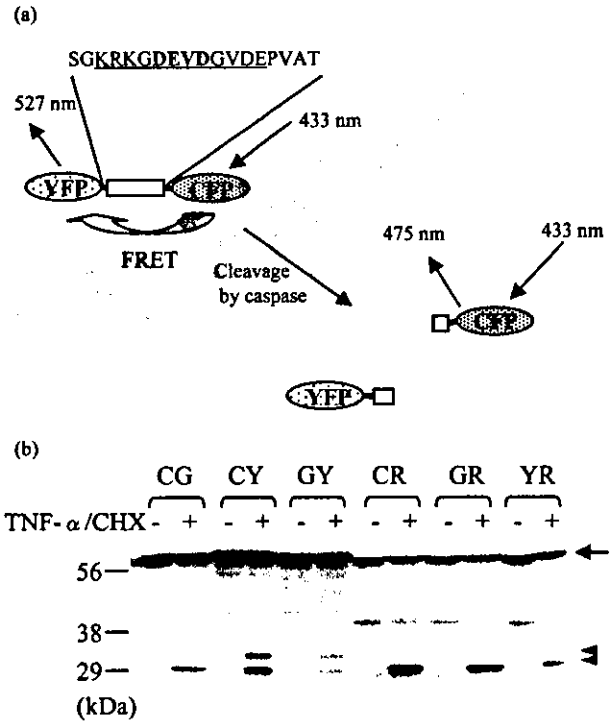

Fig. 1. Small peptide sandwiched by two different fluorescent proteins can be a caspase-sensor. a: Fusion protein that consists of a PARP-derived 12-amino-acid peptide sandwiched by CFP and YFP exhibits FRET in its intact form. In the presence of active caspases, the peptide is cleaved, and the fusion protein does not exhibit FRET. Caspase activation can be detected by measuring the fluorescence of CFP and YFP. b: Six caspase-sensors expressed in HeLa cells were cleaved by cell death stimuli. HeLa cells expressing one of the sensors were incubated in the presence or absence of TNF-α/CHX for 6 h. The arrow and arrowhead indicate the full length and cleaved fragments of the sensors.

sensor proteins in cells were extracted and analyzed by western blotting. All 6 fusion proteins were detected in their intact forms in non-treated HeLa cells (arrow in Fig. 1b), and small fragments were detected in cells treated with TNF-α/CHX (arrowhead in Fig. 1b), indicating that the fusion proteins were cleaved by cell death stimuli, as expected. The antibody used in this analysis reacts with CFP, GFP, and YFP, but not with DsRed. Therefore, CG-, CY-, and GY-sensor showed two cleaved fragments corresponding to the N- and C-terminal C/G/YFP, whereas CR-, GR-, and YR-sensor showed only one cleaved fragment corresponding to the N-terminal C/G/YFP.

Figure 2 shows the fluorescent spectra of the probes in living or dead cells. Comparing the fluorescence of living and dead cells, all sensors showed an increase of donor fluorescence and/or a reduction of acceptor fluorescence in response to cell death stimuli. This change results in a reduction of fluorescent ratio of acceptor/donor that is an index of FRET. These sensors were designed to show a reduction of FRET with caspase activation, so these results suggest that all 6 fusion proteins work as expected and can detect caspase activation as fluorescent change in living cells.

For simultaneous application of two or more fluorescent probes, minimum spectral overlap between probes is one of the important conditions. The spectra in Fig. 2 give us a clue to determine a suitable combination of probes for multi-probe analysis. CG-, CY-, or GY-sensor has the least fluorescence in the red-fluorescence region (>600 nm), so it is possible to use this fluorescent region for another dye. We can use a red-fluorescent dye that has fluorescence in this region together with CG-, CY-, or GY-sensor simultaneously. On the other hand, YR-sensor has the least fluorescence in the blue-cyan region (<500 nm), so blue-cyan-fluorescent dye is applicable with this probe for the purpose of simultaneous fluorescence imaging. The color variations of FRET probe may be useful for multi-probe analysis.

Real-time detection of caspase activation in living cells

Next, we applied the sensor proteins to real-time measurement. HeLa cells expressing one of the sensor proteins were analyzed with a time resolution of 2 min by laser-scanning confocal fluorescent microscopy. Figure 3 shows typical images (a) and fluorescent changes (b) during cell death. HeLa cells expressing GR-sensor were treated with TNF-α/CHX. An increase of donor protein fluorescence (GFP), a reduction of acceptor protein fluorescence (DsRed), and a reduction of the fluorescent ratio of acceptor/donor (DsRed/GFP) were observed in each cell at a different time. Caspases began to work at the point when the fluorescent ratio began to decrease.

All sensors showed similar changes, meaning that all sensors were useful for real-time detection of the caspase activation in a living cell, although the apparent sensitivity was different between sensors. In order to compare the sensitivity of these sensors to detect the caspase activation, the amount of the fluorescent change was calculated. We defined the start point and the end point of the reduction of the fluorescent ratio as follows:

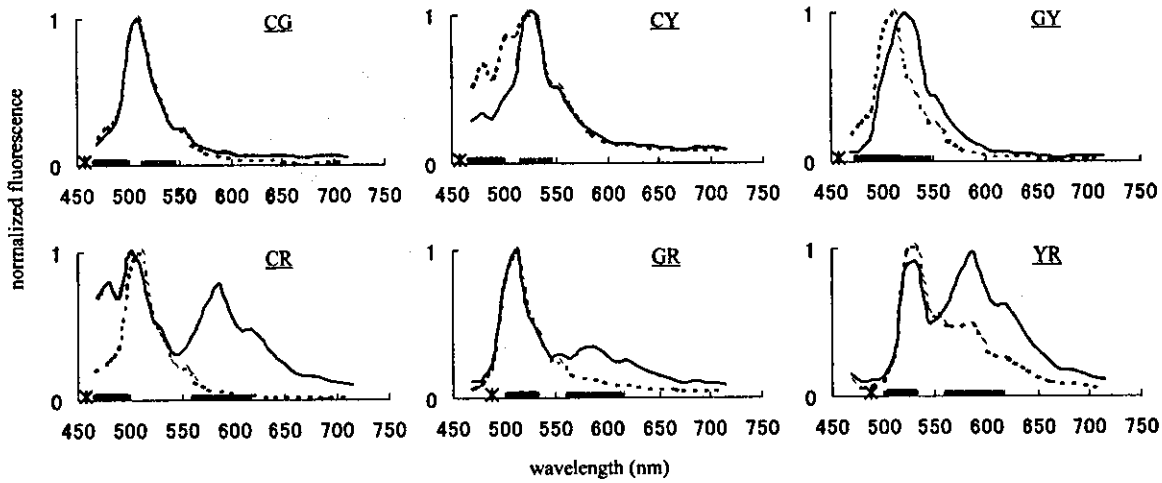

Fig. 2. Fluorescent spectra of the caspase-sensors in HeLa cells. HeLa cells expressing each sensor were treated with TNF-α/CHX for 6 h. The spectra of living cells (solid line) and dead cells (dotted line) were obtained from normal-shaped and spherical cells, respectively. Each spectrum was normalized to the peak that showed maximal intensity. The asterisks and bars on horizontal axes represent the excitation wavelength and detection range for the emitted fluorescence, respectively, used in real-time imaging analysis. Each spectrum is the average of data from 13 – 26 cells.

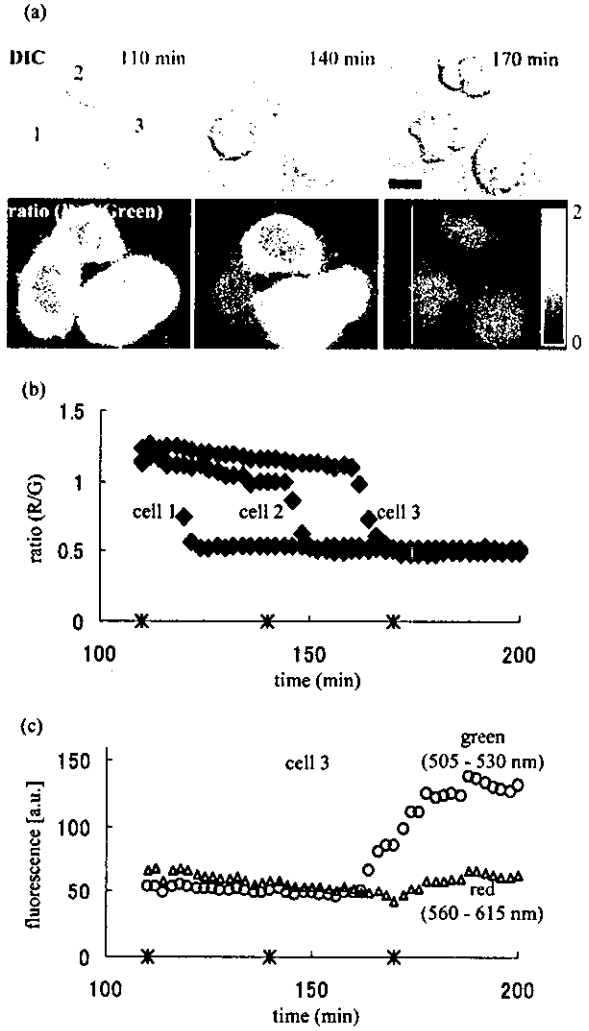

Fig. 3. Real-time imaging of caspase activation in living HeLa cells during cell death. HeLa cells expressing GR-sensor were treated with TNF-α/CHX, and fluorescent images were obtained every 2 min. a: DIC images (upper panels) and fluorescent ratios (Red/Green, lower panels) are shown in grayscale. The indicated time represents the time after the addition of TNF-α/CHX. Scale bar, 10 μm. b: The fluorescent ratio of cells were plotted. Cell 1, 2, or 3 corresponds to the cells shown in panel a. c: The mean pixel intensity in arbitrary fluorescent units (a.u.) for each channel was plotted. The fluorescence of cell No. 3 from panel a is shown. Open circle, GFP; open triangle, DsRed; closed diamond, ratio of Red/Green. Asterisks on the x-axis indicate the time points of the images in panel a.

the start point was the point after which the value decreased over four continuous points or more, the value decreased more than 10% in total, and the reduction of the value was not because of artificial noise such as focus shift; the end point followed the start point and was the point at which the value stopped decreasing. The sensitivity of the probe was calculated as $\Delta R = [(R_{end} - R_{start}) / R_{start}]$, where R_{start} and R_{end} were the fluorescent

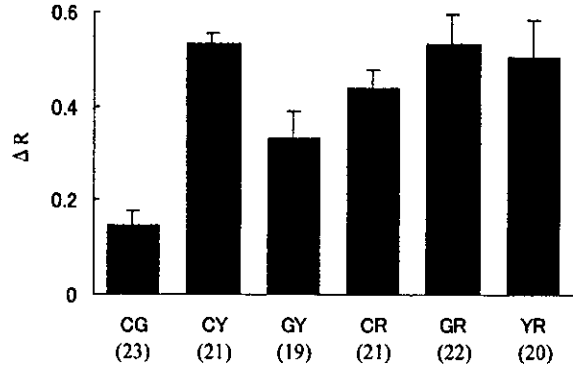

Fig. 4. Comparison of the sensitivity of various caspase-sensors. The amount of change of the fluorescent ratio during cell death (ΔR) was determined in each cell as described in the text. Bars represent means ± S.D. The number of cells used in each analysis is shown in parentheses.

ratio at the start point and the end point, respectively. Figure 4 shows ΔR for each probe. GR and YR, as well as CY, showed the highest ΔR. They each showed a more than 50% change during cell death. CR showed a slightly lower ΔR, but its change was still 44% on average. CG and GY were less sensitive, probably because the fluorescent spectra of the donor and the acceptor were so similar that our system could not effectively measure FRET between them. CY *vs* GR, CY *vs* YR, or GR *vs* YR were not significantly different, and any other comparisons were significantly different by the Games-Howell test ($P<0.05$).

Simultaneous multi-event analysis using two FRET probes

Finally, we tried to perform multi-FRET measurement. We constructed a YR-initiator caspase sensor and a CR-effector caspase sensor by changing the caspase substrate sequence in the sensor and applied them to real-time imaging analysis simultaneously in order to reveal the temporal relationships between the initiator caspase activation and the effector caspase activation in the same cell. The caspase substrate sequences were derived from procaspase-3 and PARP, respectively, and their sequences are shown in Fig. 5a. These sensors were cleaved mainly by caspase-8/9 and caspase-3, respectively (11).

Simultaneous measurement of these sensors was performed under the multi-track scanning mode, in which two sets of excitation-detection conditions were used alternatively. CFP fluorescence by excitation at 458 nm was measured in the first track, and YFP and DsRed fluorescence by excitation at 488 nm was measured in the second track. The time difference of scan-

(a) YFP-SGLDCGIETDSGVDEPVAT-DsRed : YR-(IC)sensor
CFP-SGKRKGDEVDGVDEPVAT-DsRed : CR-(EC)sensor

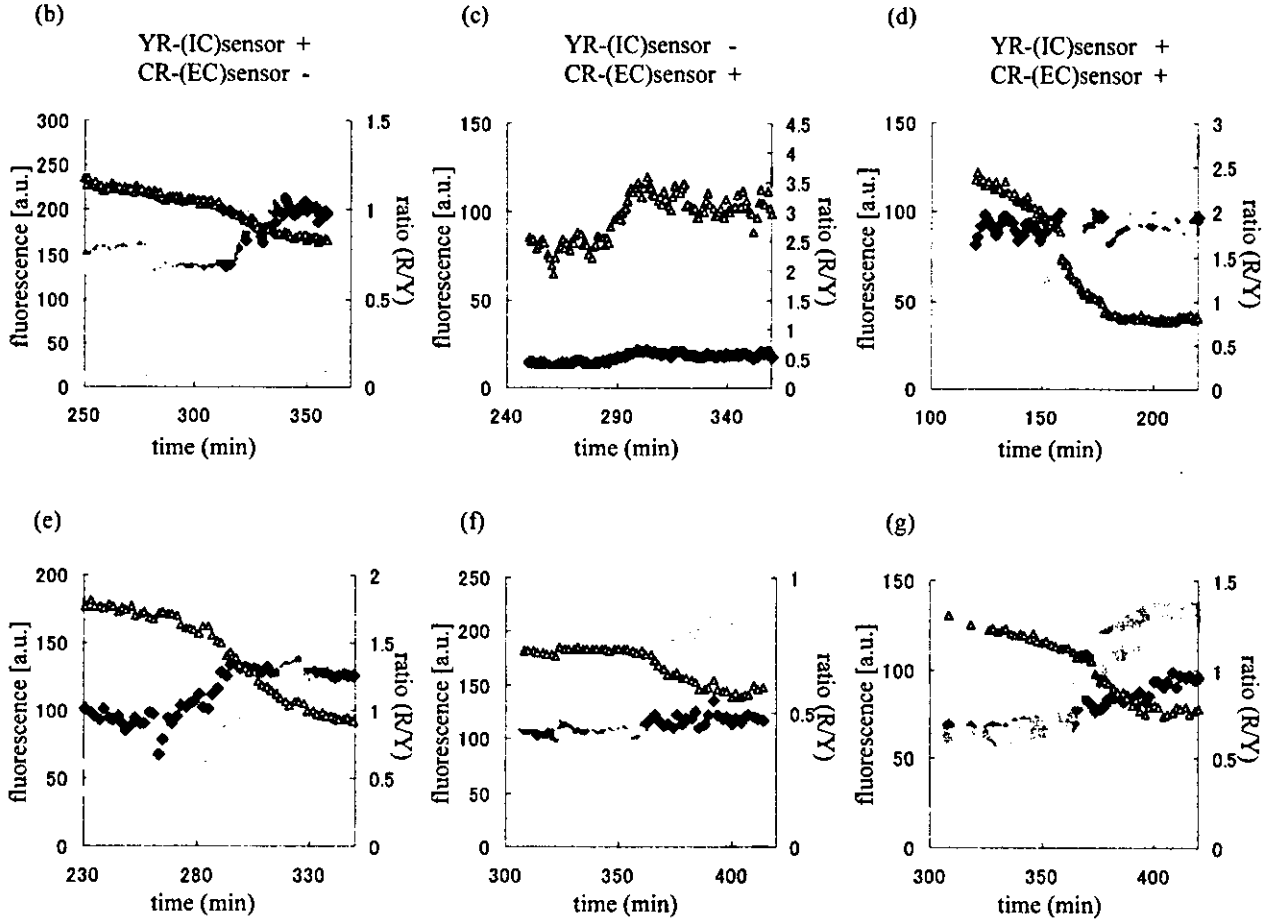

Fig. 5. Simultaneous measurement of initiator- and effector-caspase activation with YR-sensor and CR-sensor. HeLa cells expressing YR-initiator caspase sensor and/or CR-effector caspase sensor were treated with TNF-α/CHX and observed as described in the text. a: Probes used in this study. Underline indicates peptide derived from procaspase-3 and PARP, and bold indicates the consensus 4 amino acid sequence for caspase recognition. b – g: Cells expressing YR-initiator caspase sensor (b), CR-effector caspase sensor (c), or both of them (d – g) were treated with TNF-α/CHX. The fluorescence of CFP, YFP, and DsRed (colored plots) and the fluorescent ratio of DsRed/YFP (open triangles) were plotted against time after TNF-α/CHX treatment.

ning between tracks is about 3 – 8 s. Figures 5b and 5c show control studies with cells expressing only one of the probes. These control studies were conducted in the same conditions as Fig. 5d. Figures 5b and 5c indicate that the YR- and CR-sensor could detect initiator- and effector-caspase activation as an increase of YFP and CFP signal, respectively, and the contamination of the signal between the YFP and CFP channels was negligible. So, we used an increase of the YFP and CFP signal as index of the initiator- and the effector-caspase activation, respectively. The DsRed signal in Fig. 5c was derived from direct excitation of DsRed in the CR-sensor by the excitation light at 488 nm and was increased when the cell shrank because fluorescent proteins were concentrated in the cell.

Figure 5d shows typical data of multi-probe analysis with the YR-initiator caspase sensor and CR-effector caspase sensor. In this cell, the fluorescence was dramatically changed at 150 – 160 min after TNF-α /CHX treatment. The YFP and CFP signal began to increase almost simultaneously, suggesting that initiator caspase and effector caspase were initially activated within a short time period. Figures 5e – 5g show three other examples. We observed more than 30 cells in at

least 3 independent experiments and found that all dying cells showed similar results.

Discussion

In this study, we developed various color versions of caspase-sensors with CFP, GFP, YFP, and DsRed and revealed that various combinations are applicable in FRET analysis. CY, CR, GR, and YR pairs are preferable FRET pairs that possess a high ability to detect the caspase activation.

The sensitivity shown in Fig. 4 represents the apparent FRET change that depends on the measuring system and was determined by three factors. 1) Intrinsic FRET efficiency: All 4 fluorescent proteins had different fluorescent characteristics; therefore, the levels of FRET efficiency in 6 probes differed from each other. 2) Excitation crosstalk: The acceptors were excited directly by the excitation light. 3) Emission crosstalk: The acceptor channel was contaminated with the donor signal, and vice versa, because the setting shown in Table 1 could not perfectly separate the signals from the donor and the acceptor. The differences in these factors cause the difference of sensitivity among the sensors. Factors 2) and 3) reduce the apparent FRET change in the measurement. In the case of the CG-sensor, for example, fluorescent spectrum of donor and acceptor are so similar that the intrinsic FRET efficiency may be high, but excitation and emission crosstalk may also be high, much higher than in other sensors (e.g., CY-sensor), resulting in the relatively low sensitivity of this probe in our measurement system. Crosstalk effects are undesirable for detection, but it is impossible to completely eliminate these effects in the current measurement system. Maybe we could obtain different results by using spectral imaging in which emission crosstalk is eliminated (12).

According to the characteristics of the fluorescence spectrum, the CY probe seems to be one of the best for FRET-detection. However, the probe is not suitable for imaging with confocal laser microscopy, because the normal argon ion laser, the most common one in confocal microscopes, is not suitable for the excitation of CFP. The blue laser is the most suitable for the excitation, but it is not common in confocal laser microscopes. In this paper, we had to use the argon ion laser emitting 458 nm and the special emission filters optimized for the confocal ratio-imagings of caspase activation using the CY probe (11). On the contrary, the GR probe and the YR probe can be efficiently excited at 488 nm emitted by the normal argon ion laser and imaged with a set of emission filters for fluorescein and a set for rhodamine, with which almost all of the confocal microscopes are equipped. In addition, the GR probe is useful for the detection of caspase activation in flow cytometry, because almost all of the normal flow cytometers are also usually equipped with the laser and the emission filters.

DsRed-containing "red"-sensors have several characteristics that are different from other "non red"-sensors. As previously reported (13), it takes longer for DsRed to mature and emit red fluorescence than it takes for GFPs, and DsRed fluorescence tends to decrease during real-time observation, which may cause a reduction of the apparent sensitivity. These characteristics must be considered when any analysis is performed with these sensors, but as shown in Figs. 4 and 5, red-sensors have a potential similar to that of the CY-sensor and are very useful for multi-color imaging.

It has been reported that DsRed is useful as a fusion tag and a partner for FRET (13, 14). Erickson et al. analyzed the potential of DsRed as a FRET partner with CFP and GFP (14). Mizuno et al. developed a Ca^{2+} sensing fusion protein using Sapphire and DsRed (13). And recently, Karasawa et al. used two novel fluorescent proteins, namely the cyan-emitted and orange-emitted fluorescent proteins from *Acropara* sp. and *Fungia concinna*, respectively, as a FRET pair, and measured caspase-3 activity in cells (15). These results combined with our results indicate that various fluorescent proteins including GFP derivatives, DsRed, and others are useful for FRET analysis. By choosing the appropriate two fluorescent proteins as the FRET pair, we can customize the fluorescent range of FRET-based imaging probes to fit the analysis, which would expand the flexibility of simultaneous multi-event analysis.

By using the CR and YR developed in this study, we were able to analyze two FRET probes simultaneously in the same cells. In several reports, the initiator caspase activity and the effector caspase activity were measured in living cells (8, 9, 11). In these reports, however, each activity was measured independently in different cells. To our knowledge, the present study is the first report that analyzes these activities in the same cell. The results directly reveal the temporal relationships between these caspase activities. It takes a long time for cells to start the initiator caspase activation after drug treatment, but it takes a relatively short time for cells to start the effector caspase activation after the initiator caspase activation. The caspase cascade is initiated at the last stage of cell death signaling, and it proceeds within a short time period.

Acknowledgments

This study was supported in part by a Grant-in-Aid for Research on Health Sciences Focusing on Drug Innova-

tion from the Japan Health Science Foundation; a Grant-in-Aid for Research on Advanced Medical Technology from the Ministry of Health, Labour, and Welfare; and a grant (MF-16) from the Organization for Pharmaceutical Safety and Research.

References

1 Miyawaki A, Llopis J, Heim R, Mccaffery JM, Adams JA, Ikura M, et al. Fluorescent indicators for Ca^{2+} based on green fluorescent proteins and calmodulin. Nature. 1997;388:882–887.
2 Zaccolo M, Giorgi FD, Cho CY, Feng L, Knapp T, Negulescu PA, et al. A genetically encoded, fluorescent indicator for cyclic AMP in living cells. Nat Cell Biol. 2000;2:25–29.
3 Nagai Y, Miyazaki M, Aoki R, Zama T, Inouye S, Hirose K, et al. A fluorescent indicator for visualizing cAMP-induced phosphorylation in vivo. Nat Biotechnol. 2000;18:313–316.
4 Kurokawa K, Mochizuki N, Ohba Y, Mizuno H, Miyawaki A, Matsuda M. A pair of fluorescent resonance energy transfer-based probes for tyrosine phosphorylation of the CrkII adaptor protein in vivo. J Biol Chem. 2001;276:31305–31310.
5 Sato M, Ozawa T, Inukai K, Asano T, Umezawa Y. Fluorescent indicators for imaging protein phosphorylation in single living cells. Nat Biotechnol. 2002;20:287–294.
6 Tyas L, Brophy VA, Pope A, Rivett AJ, Tavaré JM. Rapid caspase-3 activation during apoptosis revealed using fluorescence-resonance energy transfer. EMBO Rep. 2000;1:266–270.
7 Rehm M, Dussmann H, Janicke RU, Tavare JM, Kogel D, Prehn JHM. Single-cell fluorescence resonance energy transfer analysis demonstrates that caspase activation during apoptosis is a rapid process: role of caspase-3. J Biol Chem. 2002;277: 24506–24514.
8 Luo KQ, Yu VC, Pu Y, Chang DC. Measuring dynamics of caspase-8 activation in a single living HeLa cell during TNFα-induced apoptosis. Biochem Biophys Res Commun. 2003;304: 217–222.
9 Takemoto K, Nagai T, Miyawaki A, Miura M. Spatio-temporal activation of caspase revealed by indicator that is insensitive to environmental effects. J Cell Biol. 2003;160:235–243.
10 Tsien RY. The green fluorescent protein. Annu Rev Biochem. 1998;67:509–544.
11 Kawai H, Suzuki T, Kobayashi T, Mizuguchi H, Hayakawa T, Kawanishi T. Simultaneous imaging of initiator/effector caspase activity and mitochondrial membrane potential during cell death in living HeLa cells. Biochim Biophys Acta. 2004;1693:101–110.
12 Zimmermann T, Rietdorf J, Pepperkok R. Spectral imaging and its applications in live cell microscopy. FEBS Lett. 2003;546: 87–92.
13 Mizuno H, Sawano A, Eli P, Hama H, Miyawaki A. Red fluorescent protein from Discosoma as a fusion tag and a partner for fluorescence resonance energy transfer. Biochemistry. 2001; 40:2502–2510.
14 Erickson MG, Moon DL, Yue DT. DsRed as a potential FRET partner with CFP and GFP. Biophys J. 2003;85:599–611.
15 Karasawa S, Araki T, Nagai T, Mizuno H, Miyawaki A. Cyan-emitting and orange-emitting fluorescent proteins as a donor /acceptor pair for fluorescence resonance energy transfer. Biochem J. 2004;381:307–312.

Available online at www.sciencedirect.com
SCIENCE DIRECT
Biochimica et Biophysica Acta 1693 (2004) 101–110
BIOCHIMICA ET BIOPHYSICA ACTA
BBA
www.bba-direct.com

Simultaneous imaging of initiator/effector caspase activity and mitochondrial membrane potential during cell death in living HeLa cells

Hiroshi Kawai[a,*], Takuo Suzuki[a], Tetsu Kobayashi[a], Hiroyuki Mizuguchi[b], Takao Hayakawa[a], Toru Kawanishi[a]

[a] *Division of Biological Chemistry and Biologicals, National Institute of Health Sciences, 1-18-1 Kamiyoga, Setagaya, Tokyo 158-8501, Japan*
[b] *Division of Cellular and Gene Therapy Products, National Institute of Health Sciences, Tokyo 158-8501, Japan*

Received 26 January 2004; received in revised form 19 May 2004; accepted 28 May 2004
Available online 1 July 2004

Abstract

A family of cystein proteases, the caspases, plays a central role in mediating cell death. In this study, we measured the activation of the initiator and effector caspase in real time, and studied the relationship between caspase activity and mitochondrial membrane potential in living cells by means of bioimaging. We also designed and developed a fluorescence resonance energy transfer (FRET)-based genetically encoded fluorescent indicator, which consisted of yellow fluorescent protein (YFP), a peptide sequence which can be cleaved by specific caspases, and cyan fluorescent protein (CFP). Two peptide sequences which could be cleaved by initiator caspases and effector caspases, respectively, were used. Simultaneous real-time measurements of the caspase activity and mitochondrial membrane potential in the cells treated with TNF-α and staurosporine revealed that dying cells showed caspase activation and mitochondrial depolarization, and that these events, however, were not firmly linked. Although it takes anywhere from 1 to over 10 h after the addition of the cell death inducer for the caspases to begin to be activated, initiator caspases and effector caspases are activated within a short period of time at the last stage in the entire process leading to cell death.

Keywords: Cell death; Caspase; Mitochondrial depolarization; Imaging; GFP; Confocal fluorescent microscopy

1. Introduction

Apoptosis is an essential process for excluding damaged or harmful cells and maintaining homeostasis in biological systems. The disruption of this process is assumed to cause various diseases, including cancer, autoimmune diseases, and neurodegenerative diseases. Apoptosis can be induced experimentally by such stimuli as UV irradiation, growth factor withdrawal, death receptor ligands, or cytotoxic drugs. These factors induce cell death via a cascade of protease activation. These proteases are cystein proteases called caspases. They play a central role in the apoptotic cell death machinery [1,2]. Caspases are synthesized as proprotein, which is processed to its matured form and exerts its catalytic activity at the proper time. For a better understanding of cell death and the diseases that result from it, it is important to elucidate the mechanism of caspase activation.

The caspases are divided into two groups, initiator caspases (e.g., caspase-8, -9, -10) and effector caspases (e.g., caspase-3, -6, -7). The initiator caspases act at an earlier stage of cell death, and activate the effector caspases by hydrolytic cleavage [3–9]. The effector caspases cleave various substrates such as lamin, poly(ADP-ribose)polymerase (PARP), and DNA fragmentation factor (DFF), which cause biochemical and morphological changes in cells, and finally bring about cell death [10,11]. For example, tumor necrosis factor (TNF)-α, a well-known apoptosis inducer, activates caspase-8 through signal transduction via the TNF receptor, which is one of the death receptors [3–7,12]. Caspase-8 then cleaves and activates caspase-3, which cleaves various substrates and causes apoptotic cell death.

* Corresponding author. Tel.: +81-3-3700-9084; fax: +81-3-3700-9084.
E-mail address: kawai@nihs.go.jp (H. Kawai).

0167-4889/$ - see front matter © 2004 Elsevier B.V. All rights reserved.
doi:10.1016/j.bbamcr.2004.05.009

However, some cell death inducers, e.g., staurosporine, exert their activity without binding to the death receptor. Mitochondria play a pivotal role in this pathway [8,9,13]. Mitochondrial membranes are affected by the cell death signal, and cytochrome *c* (cyt. *c*) and other apoptosis-related factors are released to cytosol. Cyt. *c* forms a protein complex called apoptosome with Apaf-1 and procaspase-9. Procaspase-9 is processed and activated in apoptosome, and active caspase-9 cleaves caspase-3 to its active form. Previous studies have identified various caspases and revealed their roles in cell death machinery. But how each reaction proceeds, and how these reactions relate to other cellular events during cell death in living cells, has not been thoroughly investigated.

Green fluorescent protein (GFP) and its variants are widely used in biological studies [14]. They are used not only as a fluorescent tag to visualize a certain protein, but also to monitor the dynamic changes of intracellular signals, e.g., Ca^{2+}, IP_3, protein kinase activities, and proteolysis [15–26]. Some of these biological studies used the fluorescent resonance energy transfer (FRET) between cyan fluorescent protein (CFP) and yellow fluorescent protein (YFP) [27]. CFP and YFP were linked with a small peptide and/or functional protein(s), which changed their conformation by means of a certain cellular signal. This conformational change affected the FRET efficiency of the probe, because FRET efficiency relates to the distance and angle between two fluorophores. Since the FRET efficiency can be estimated by the fluorescence ratio of YFP and CFP (YFP/CFP), the change in the intracellular signal can be detected by measuring the CFP and YFP fluorescence. Bioimaging with a fluorescent probe and fluorescence microscopy makes it possible to detect very subtle and rapid signals in living cells, which is otherwise impossible, and to reveal the temporal and spatial relationships between these signals.

Several groups have already developed probes for caspase activity and have monitored the caspase activities in single cells [28–34]. Almost all of these researchers, however, studied only effector caspase or caspase-3. In this study, we tried to monitor the activity of initiator and effector caspases by means of real-time bioimaging, and investigated the relationship among the caspase activation, mitochondrial membrane potential, and morphological changes during cell death. Recently, Ohnuki et al. [32] reported a fluorescent probe for caspase-8, and studied the relationship between caspase-8 activation and β-amyloid toxicity. Takemoto et al. [33] and Luo et al. [34] developed a fluorescent probe for caspase-9 and caspase-8, and carried out real-time imaging. We used a strategy similar to theirs to develop the probe, but our report is the first to show the relationship between initiator caspase activation and mitochondrial depolarization. Because both of these events are important in cell death machinery, clarifying their temporal relationship by simultaneous imaging is a significant step.

2. Materials and methods

2.1. Plasmid construction

Plasmid encoding YFP-CFP was generated by PCR with pECFP-C1 and pEYFP-C1 (Clontech, Palo Alto, CA). The sequence encoding 11 amino acids at the C-terminus of YFP was eliminated in this construct. The linker connecting YFP and CFP was identical with the multi cloning site of pEYFP-C1. This construct was cloned in the *Nhe*I–*Not*I site of pEGFP-N1 vector. The oligonucleotides encoding the respective caspase's substrate sequence were inserted into the *Bsp*EI–*Age*I site, and the oligonucleotide encoding His_{10} followed by a stop codon (TAA) was inserted into the *Bsr*GI–*Not*I site at the C-terminus of CFP. One caspase substrate sequence was derived from procaspase-3 (5′-CCGGACTGGACTGTGGCATTGAGACAGACAGTGGTGTTGATGAA-3′ and 5′-CCGGTTCATCAACACCACTGTCTGTCTCAATGCCACAGTCCAGT-3′), and another was derived from PARP (5′-CCGGAAAGAGAAAAGGCGATGAGGTGGATGGAGTGGATGAA-3′ and 5′-CCGGTTCATCCACTCCATCCACCTCATCGCCTTTTCTCTTT-3′) [35,36]. The His_{10} sequence was made from the following oligonucleotides, 5′-GTACAAGCACCACCACCACCACCACCACCACCACCACTAAAGC-3′ and 5′-GGCCGCTTTAGTGGTGGTGGTGGTGGTGGTGGTGCTT-3′. The amino acid sequences between YFP and CFP are shown in Fig. 1. Oligonucleotides were provided by Hokkaido System Science Co. (Sapporo, Japan). All cloned sequences were verified by sequencing.

2.2. Cell culture and transfection

HeLa cells were cultured in DMEM (Sigma-Aldrich, St. Louis, MO) supplemented with 100 units/ml of penicillin G, 100 μg/ml of streptomycin and 10% fetal calf serum (GIBCO). Plasmid encoding the fusion protein was transfected into HeLa cells using Effectene Transfection Reagent (QIAGEN, Hilden, Germany) according to the manufacturer's instructions. After 12–24-h incubation with the transfection reagent, the cells were washed with PBS and cultivated on dishes suitable for assay in medium containing 500 μg/ml of G418 for an additional 1–3 days until the assay was performed.

2.3. Extraction and purification of the fusion proteins

Cells expressing the fusion protein were cultured in 60-mm plastic dishes. The cells were washed with PBS and lysed with 20 mM Tris–HCl buffer (pH 7.9) containing 0.5 M NaCl, 5 mM imidazole and 1% Triton X-100. The lysate was centrifuged at 10,000 × *g* for 10 min at 4 °C and filtered with a 0.45-μm filter. The fusion protein that contained His_{10} was purified with His-Bind Resin (Novagen, Madison, WI) by following the manufacturer's

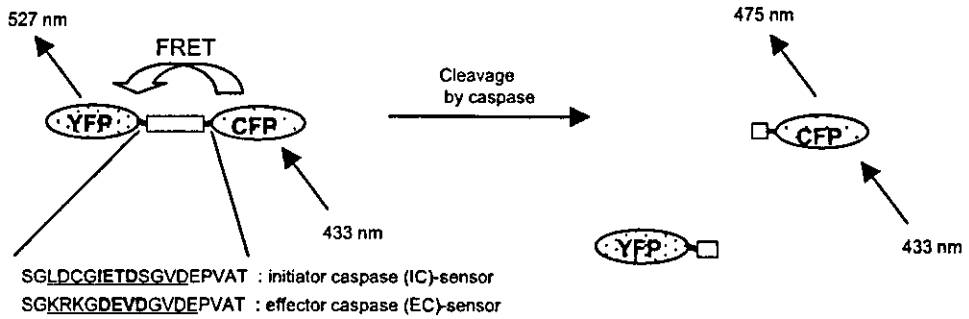

Fig. 1. The probe protein consists of YFP, a substrate peptide of caspase, and CFP. When excited at 433 nm (excitation max. of CFP), this fusion protein shows FRET and emits fluorescence at 527 nm (emission max. of YFP) if the protein is intact. If there are active caspases, the fusion proteins are cleaved, FRET does not occur, and this fusion protein emits fluorescence at 475 nm (emission max. of CFP). The emission ratio of YFP/CFP indicates the caspase activity around the probe protein. The linker region between YFP and CFP consists of 18 amino acids. The sequences derived from procaspase-3 (IC-sensor) and PARP (EC-sensor) are underlined, and the site of consensus recognition by [the] caspase are shown in bold face.

instructions with slight modifications. We used 20 mM imidazole solution instead of 60 mM imidazole solution to wash the resin after loading the sample. Purified fusion proteins were obtained in 20 mM Tris–HCl buffer (pH 7.9) containing 0.5 M NaCl and 1 M imidazole. The solvent was changed to other buffers by centrifugation tube with a MW 30,000 cutoff filter (Millipore, Bedford, MA) if necessary.

2.4. Western blotting

Cells cultured in a plastic dish were washed with PBS and lysed with 1 × SDS loading buffer, or extracted protein sample was mixed with the same amount of 2 × SDS loading buffer. The samples dissolved in 1 × SDS loading buffer were incubated at 95 °C for 2 min, and then they were loaded onto SDS-polyacrylamide gels (10%). Proteins were separated at 20 mA and then blotted to PVDF membranes in Tris–glycine transfer buffer at 100 V for 2 h. The membrane was incubated with block ace (Dainippon Pharmaceutical, Osaka, Japan) for 1 h, anti-GFP monoclonal antibody (Clontech, diluted with 0.1 × block ace to 1:10,000) for 1–2 h, and anti-mouse IgG horseradish peroxidase-conjugated secondary antibody (Chemicon International Inc., Temecula, CA, diluted with 0.1 × block ace to 1:10,000) for 1 h. The membrane was washed with TBS-T two to three times for 5 min after the incubation with the antibody. All of these incubations were performed at room temperature. The membrane was developed with the ECL chemiluminescence detection reagent (Amersham Biosciences, Piscataway, NJ).

2.5. Measurement of fluorescence

The fluorescence of the fusion protein purified by His-Bind Resin was measured using a HITACHI F-310 fluorometer. Fluorescent spectra were scanned from 450 to 550 nm with a scanning speed of 120 nm/min after excitation at 433 nm by Hg lamp.

2.6. Cleavage of the fusion proteins by active caspases

Recombinant human active caspase-1 through caspase-10 were purchased from BioVision (Mountain View, CA). The purified fusion protein dissolved in 1 × Reaction Buffer (BioVision) was incubated with 1 unit of the respective active caspase at 37 °C for 1 h. One unit of the active caspase is the enzyme activity that cleaves 1 nmol of the individual substrate (YVAD-pNA for 1, VDVAD-pNA for 2, DEVD-pNA for 3 and 7, WEHD-pNA for 4 and 5, VEID-pNA for 6, IETD-pNA for 8 and 10, and LEHD-pNA for 9), per hour at 37 °C. Reactions were terminated by adding 2 × SDS loading buffer and subjected to SDS-PAGE and Western blotting.

2.7. Bioimaging with fluorescent microscopy

Transfected cells were cultured on a cover glass (25-mm diameter, 0.15–0.18-mm thickness) for 1–3 days. Cells were treated with TNF-α (200 ng/ml, dissolved in PBS) or staurosporine (3 μM, dissolved in DMSO), and then incubated under the usual culture condition for 1–2 h before analysis. Tetramethylrhodamine methyl ester (TMRM, 50 nM, dissolved in DMSO) was added 20–30 min before the analysis if mitochondrial membrane potential was to be measured. Analyses were carried out by confocal laser scanning fluorescent microscopy using a Carl Zeiss LSM510 system. During the observation, the media were buffered with 10 mM HEPES buffer (pH 7.4) and the cells were maintained at 35–37 °C. DIC images and grayscale images for fluorescence channels were obtained every 2 min unless otherwise described. Excitation lights for the FRET probe (458 nm) and TMRM (543 nm) were provided by an Ar laser with a 458 dichroic mirror and a HeNe laser with a 543 dichroic mirror, respectively. Images of the FRET probe were obtained separately for both cyan and yellow fluorescence using a 515 dichroic mirror and a BP467.5–497.5 emission filter for the cyan and a BP515–545 emission filter for the yellow. Images of TMRM were obtained using a

LP560 emission filter. At first, we tried a BP475–515 filter and a LP515 filter, which were loaded as a standard set in LSM510, for cyan and yellow fluorescence, respectively, but this setting was not suitable for our experiments for several reasons. First, the cyan fluorescence obtained through the BP475–515 filter was too weak, and second the LP515 filter cannot exclude the possibility that TMRM-derived fluorescence contaminated the channel for yellow fluorescence. We prepared several emission filters, and obtained the best results using the setting described above. Contamination of the fluorescence between the channels was negligible in this condition (data not shown). Images were processed and quantified using MetaFluor software. The fluorescent intensity of the whole cell area was used in this analysis. As cells changed their morphology during the observation, the whole cell areas were determined separately in each image.

3. Results

3.1. Design of the probes

We designed and developed a FRET-based genetically encoded fluorescent indicator, which consisted of YFP, a peptide sequence which can be cleaved by specific caspases, and CFP. Since FRET efficiency depends on the distance between CFP and YFP, this fusion protein should show FRET, which can be significantly reduced when the peptide sequence is cleaved by active caspases (Fig. 1). We used two peptide sequences, which were 12 amino acids in length and contained a caspase recognition site in the middle. One was derived from procaspase-3, and was expected to be cleaved by caspase-8/9/10, and the other was from PARP, and was expected to be cleaved by caspase-3/6/7. These probes, which we named the initiator caspase (IC)-sensor and effector caspase (EC)-sensor, were able to indicate the cleavage of procaspase-3 and PARP; in other words, they were able to indicate the protease activities of the initiator caspases and effector caspases, respectively.

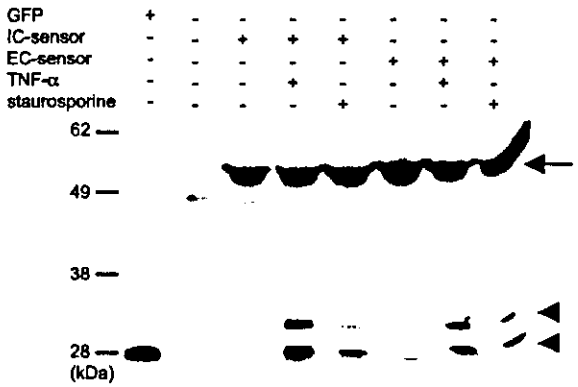

Fig. 2. Expression and cleavage of the probe proteins in HeLa cells. HeLa cells transfected with plasmid encoding IC-sensor (lanes 3–5) or EC-sensor (lanes 6–8) were exposed with 200 ng/ml of TNF-α (lanes 4 and 7) or 3 μM of staurosporine (lanes 5 and 8) for 6 h. The cell lysate of each experiment was prepared and analyzed by Western blot analysis with anti-GFP monoclonal antibody. A control experiment (non-transfected, non-treated HeLa cells, lane 2) shows no band. Lane 1 shows recombinant GFP as a reference. The arrow and arrowheads indicate intact and cleaved YFP-peptide-CFP, respectively.

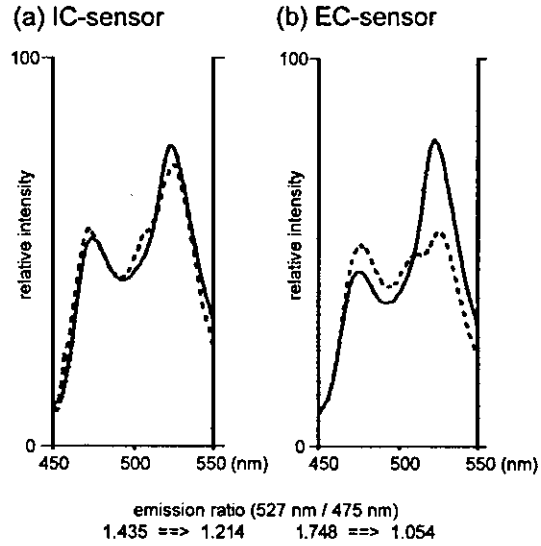

Fig. 3. The fluorescent changes by the cell death stimuli. HeLa cells expressing the IC-sensor or EC-sensor were incubated in the presence or absence of 200 ng/ml of TNF-α for 6 h. The probe protein was extracted and purified as described in Section 2, and the fluorescent spectra with excitation at 433 nm were measured. The fluorescent spectra of the IC-sensor (a) and EC-sensor (b) from non-treated cells (solid line) and TNF-α-treated cells (dotted line) are shown.

3.2. Characterization of the probe proteins in living cells

HeLa cells expressing one of the probe proteins were treated with a cell death inducer, consisting of either 200 ng/ml of TNF-α or 3 μM of staurosporine. After 6 h of exposure, the cells were lysed and underwent Western blot analysis. As shown in Fig. 2, both probe proteins were detected from the transfected HeLa cells (lanes 3–8), and the 25–30-kDa fragments were detected from the cells treated with TNF-α (lanes 4 and 7) or staurosporine (lanes 5 and 8). These fragments were identical to the cleaved fragments (YFP-cleaved peptide and cleaved peptide-CFP-His_{10}). Both the IC-sensor and EC-sensor are successfully expressed in HeLa cells, and are cleaved in cells by cell death stimuli.

The fluorescent spectra of the probe proteins were measured after purification with a His tag. Fig. 3 shows the fluorescent spectra of the IC-sensor (a) and EC-sensor (b) from the TNF-α-treated and non-treated (control) HeLa cells expressing one of the probe proteins. The probe proteins from the control cells showed spectra with two emission peaks at 475 and 527 nm by excitation at 433 nm

(solid line in Fig. 3(a) and (b)). These peaks were identical to those of CFP and YFP, respectively. The probe protein from the TNF-α-treated cells also showed spectra with two peaks, but compared with the non-treated control, the emission at 475 nm was enhanced, and that at 527 nm was reduced (dotted line in Fig. 3(a) and (b)). This result is likely due to the cleavage of the probe protein by caspases, which reduce the energy transfer from CFP to YFP. The ratio of the emission intensity (527/475 nm) was reduced by about 20–40% by the TNF-α treatment in this assay. The staurosporine treatment produced the same results as the TNF-α treatment (data not shown).

YFP can be excited directly by excitation light at 433 nm, and, therefore, YFP fluorescence itself is not an indicator for FRET. We measured the fluorescent ratio, and showed that the ratio was reduced by cell death stimuli, indicating that FRET from CFP to YFP was reduced. The fluorescent ratio can be an indicator for FRET, and the reduction of the ratio indicates the activation of the caspases. We used the fluorescent ratio as the indicator for caspase activation in the following experiments.

3.3. Cleavage of the fusion protein by recombinant caspase

In a cell-free system, we investigated which caspase could cleave IC- and EC-sensors to confirm the specificity of the probe proteins. The probe protein purified from a HeLa cell lysate was incubated with human recombinant caspase-1–10, and Western blotting with an anti-GFP antibody was used to confirm whether the probe protein was cleaved by the respective caspases. Fig. 4 shows the results. The IC-sensor was cleaved by caspase-8 and caspase-9, and slightly by caspase-5 and caspase-6. The bands for the cleaved probe proteins were quantified, and the activities of caspase-8 and -9 were estimated to be 5–10 times higher than that of caspase-5 and -6. The EC-sensor was cleaved by caspase-3, and slightly by caspase-7, -8, and -9. The caspase-3 activity was more than 10 times higher than the activity of the other caspases. Although we cannot exclude the possibility that some caspases can cleave the probes in living cells despite their inability to cleave them in this cell-free system, or that some proteases other than caspase-1–10 can cleave them, these results clearly showed that the IC- and EC-sensor proteins could mainly detect the caspase-8/9 activity and caspase-3 activity, respectively.

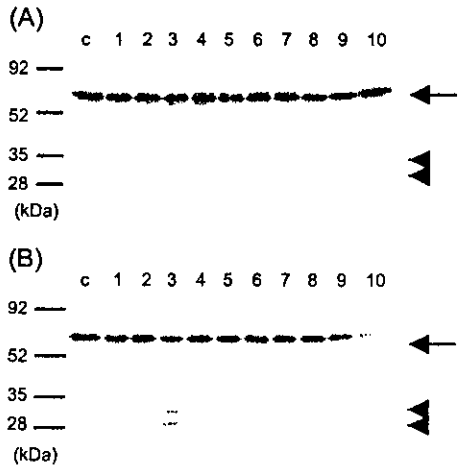

Fig. 4. Selective cleavage of the probe proteins by certain caspases. The probe protein was incubated with recombinant active caspase-1–10 at 37 C for 1 h. The resultants were analyzed by Western blotting with anti-GFP monoclonal antibody. (A) IC-sensor; (B) EC-sensor. Numbers 1–10 represent the results from assays with caspase-1–10, respectively, and c represents the control experiment in which the assay was performed in the absence of caspase. The arrow and arrowheads indicate intact and cleaved sensor proteins, respectively.

3.4. Simultaneous bioimaging of caspase activity and mitochondrial membrane potential

Next, we tried to carry out real-time detection of the caspase activity and mitochondrial membrane potential in single living cells. HeLa cells were transfected with the caspase-sensor and treated with 50 nM of TMRM, a mitochondrial membrane potential-indicator. It has been reported that TMRM is less toxic than tetramethylrhodamine ethyl ester, and does not inhibit mitochondrial respiration at this dose [37]. The caspase activity and mitochondrial membrane potential were simultaneously measured in living cells every 2 min by confocal laser-scanning fluorescent microscopy, as described in Section 2. A control study in which the cells were treated with solvent (DMSO, 1%) did not show any fluorescent or morphological changes (data not shown).

Fig. 5 shows typical images of the assay. Cells expressing the IC-sensor were treated with 200 ng/ml of TNF-α (a) or 3 μM of staurosporine (b). After 1–6-h exposure, changes were observed in some cells. The fluorescence of the CFP channel increased, while that of the YFP channel decreased (not shown in Fig. 5; see Fig. 6), and the emission ratio of YFP/CFP, which represents the FRET efficiency, dramatically decreased, indicating that the caspases were activated. The fluorescence of TMRM also decreased, indicating that the mitochondrial membrane potential was reduced. As previously reported by other groups, the timing of the response differs in each cell [28–30,33,34]. Since several reports suggested that the induction of apoptosis is related to the cell cycle, the difference of timing we observed here might depend on which cell-cycle phase the individual cells were in [38,39].

3.5. Morphology during cell death induced by TNF-α or staurosporine

There were differences in morphology between the TNF-α-treated and staurosporine-treated cells. The TNF-α-treated cells shrank drastically when the caspase was activated, whereas the staurosporine-treated cells did not show such obvious changes in morphology, although the caspases were

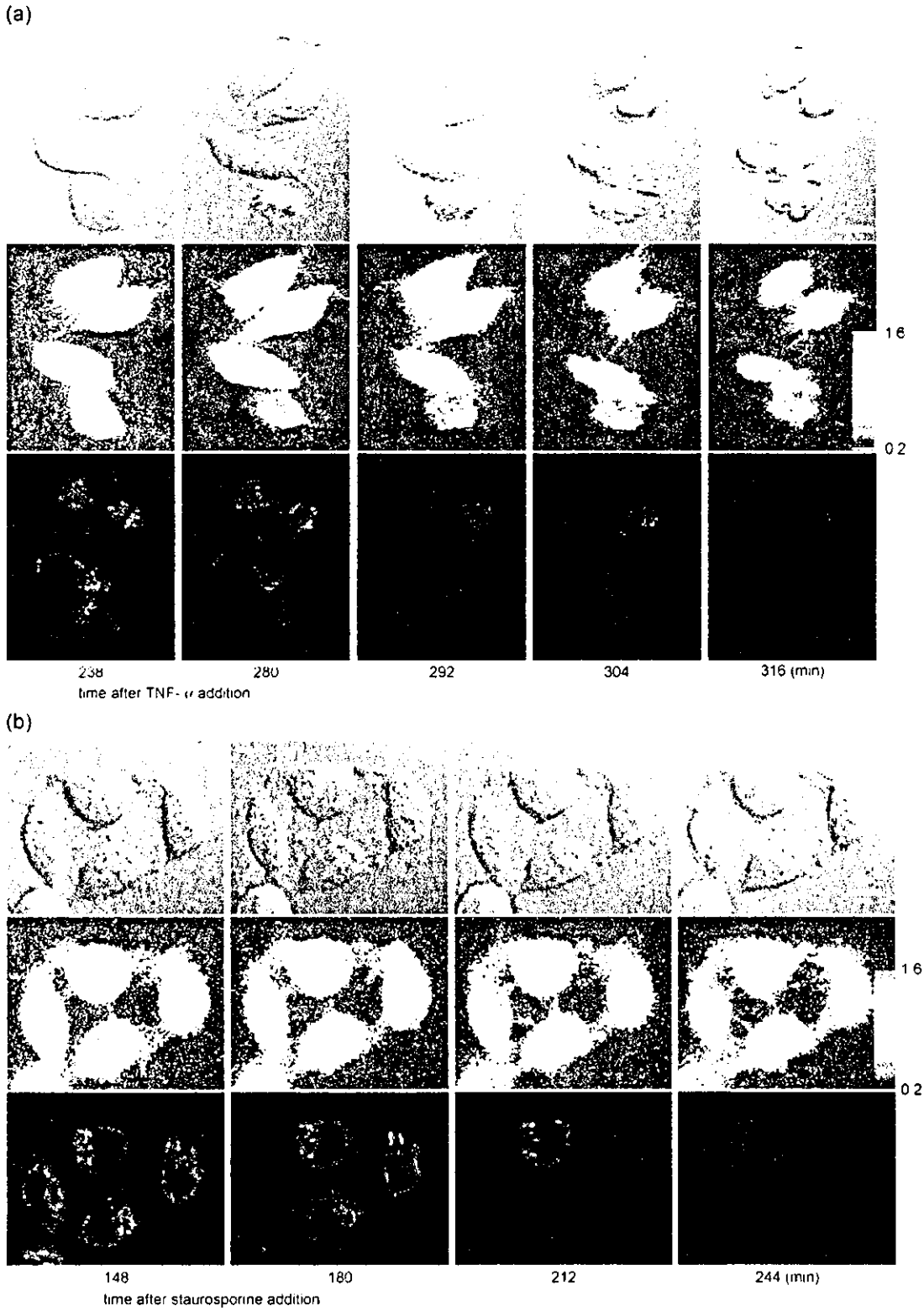

Fig. 5. Time lapse images of the caspase activity and the mitochondrial membrane potential obtained by LSM510. HeLa cells expressing the IC-sensor were incubated with 200 ng/ml of TNF-α (a) or 3 μM of staurosporine (b). The cells were then observed by confocal microscopy, and DIC and fluorescent images were obtained at 2-min intervals, as described in Section 2. DIC images (upper panels), the emission ratio of YFP/CFP (middle panels), and the fluorescent intensity of TMRM (lower panels) at the indicated time are shown in pseudo colors. The reduction of the YFP/CFP ratio represents caspase activation, and the reduction of TMRM fluorescence represents the reduction of the mitochondrial membrane potential. The bars in the upper right images indicate 10 μm.